Sustainable Food Technology

ROYAL SOCIETY OF CHEMISTRY

PAPER

View Article Online
View Journal

Cite this: DOI: 10.1039/d5fb00743g

An antibacterial γ-CD-MOF complex functionalized film for fish meat safety and freshness

Meimei Guo,[a] Tahirou Sogore,[a] Jin Huang,[a] Xinyu liao,[c] Mofei Shen*[b] and Tian Ding *[ac]

In this study, we developed a functionalized film for packaging refrigerated fish fillets. The functionalized film was produced using a γ-cyclodextrin metal–organic framework (γ-CD-MOF) loaded with gold nanoparticles (γ-CD-MOF complex), with polydimethylsiloxane serving as the substrate. The obtained functionalized film significantly enhanced antioxidant activity, demonstrating a 44% 2,2-diphenyl-1-picrylhydrazyl radical ($DPPH^{\bullet+}$) scavenging rate and a 58% 2,2′-azino-bis(3-ethylbenzothiazoline-6-sulfonic acid) radical ($ABTS^{\bullet+}$) scavenging rate, much higher than those of the pure film. Furthermore, the functionalized film reduced the bacterial counts of *Escherichia coli* O157:H7 (*E. coli* O157:H7) by approximately 99.4% and *Staphylococcus aureus* (*S. aureus*) by approximately 80% within 24 hours. Moreover, the functionalized film maintained the pH within 6.70 ± 0.02 and the volatile basic nitrogen (TVB-N) value within 8.71 mg/100 g on day 4. It also exhibited a lower total viable count (TVC) value compared to both the control and pure film groups during the first four days, significantly improving the storage safety of refrigerated fish meat. Additionally, the embedded γ-CD-MOF complex affected the tensile strength, water contact angle, and water vapor transmission rate (WVTR) of the functionalized film. In conclusion, this functionalized film increased the shelf life of refrigerated fish fillet samples by inhibiting microbial growth and reducing the oxidation rate, compared to the control sample.

Received 27th October 2025
Accepted 3rd December 2025

DOI: 10.1039/d5fb00743g

rsc.li/susfoodtech

Sustainability spotlight

This study drives sustainable food packaging innovation by tackling fish spoilage and eco-harmful nanoparticle synthesis. We develop a functionalized film using a γ-CD-MOF (a biocompatible, "edible" material from γ-cyclodextrin and alkali metals) for *in situ* gold nanoparticle synthesis, requiring no toxic surfactants/stabilizers needed and thereby avoiding hazards of traditional methods and limitations of biological synthesis. With polydimethylsiloxane (low-cost, stable, inert) as the substrate, the film delivers dual value: its strong antioxidant/antimicrobial properties reduce fish TVB-N, pH, and TVC, cutting spoilage-related food waste (meat products often lose up to 40% of production). Its biocompatible components also minimize post-use environmental impact, outperforming conventional packaging. By integrating green synthesis, seafood waste reduction, and safe packaging, this research aligns with SDG 12 (Responsible Consumption and Production) and supports aquatic product sustainability, offering a practical path for eco-friendly food packaging.

1 Introduction

Ensuring the safety and quality of food products during storage is a critical issue for both industries and governments. Meat products, in particular, are highly susceptible to spoilage, with up to 40% of production potentially lost.[1,2] Fish is a rich source of high-quality protein, providing essential amino acids, minerals, and highly unsaturated fatty acids.[3] These nutrients are crucial for human nutrition and digestive processes. However, during the postmortem stage of fish, the various nutrients within the tissue undergo enzymatic and microbial degradation, resulting in the formation of new chemical compounds, such as reactive aldehydes and other degradation by-products. These compounds are primarily responsible for the spoilage process of fish.[4] As such, fish with an extended shelf life is essential for both producers and consumers.

Fish processing and preservation techniques have been developed to inhibit or slow microbial growth. Recently, nanocomposite films incorporating antimicrobial agents such as essential oils, bacteriocins, antimicrobial enzymes, or metal nanoparticles have been developed. Metal nanoparticles are widely recognized for their promising antimicrobial properties, owing to their small size and high surface area-to-volume ratio, which provide an extensive reactive surface capable of interacting effectively with microorganisms.[5] They can be readily integrated with other biomaterials to enhance antibacterial activity.[6] For example, CuO nanoparticle complexes have been incorporated into polylactic acid/poly(butylene adipate-*co*-terephthalate)

[a]*College of Biosystems Engineering and Food Science, Zhejiang University, Hangzhou, 310058, China. E-mail: tding@zju.edu.cn*

[b]*Department of Food Science and Engineering, Zhejiang University of Technology, Hangzhou, Zhejiang 310014, China. E-mail: mfshen@zjut.edu.cn*

[c]*Innovation Center of Yangtze River Delta, Zhejiang University, Jiaxing, 314102, China*

composite films and used for antimicrobial food packaging materials.[7] A silver–carrageenan (Ag/Carr) nanocomposite film for food packaging was reported. The antimicrobial properties of the synthesized films were explored, and these films were employed for the storage of cottage cheese (dairy product) and strawberries (fruit).[8] Additionally, antimicrobial composite films for fruits containing ZnGlu MOF particles have been reported, with jasmine essential oil as the active component incorporated into the MOF channels.[9] Furthermore, gold, silver, copper, cobalt, indium, tungsten, tin, aluminum, chromium, zinc, manganese, tantalum, and titanium-based nanoparticle thin films are reported to have good antimicrobial activity.[10–12] Among these metal nanoparticles, gold nanoparticles have garnered significant interest from researchers due to their low toxicity and excellent biocompatibility.[13]

Gold nanoparticles are generally synthesized *via* physicochemical and biological methods, but both have limitations: the former uses hazardous/toxic substances, harming health and the environment;[14] the latter is restricted by limited biomaterials, long synthesis, poor organism regulation, and large particle size variability.[15] Therefore, in this study, gold nanoparticles were green-synthesized *in situ* using a γ-CD-MOF, which is composed of γ-cyclodextrin and alkali metal ions (*e.g.*, K^+). As a biocompatible multifunctional material with permanent porosity, the γ-CD-MOF not only contains abundant hydroxyl groups but also features –OCCO– binding groups on its primary and secondary faces, enabling complexation with metal ions. Additionally, its porous structure allows absorption of guest molecules (*e.g.*, nanoparticles), collectively supporting the *in situ* green synthesis without the need for additional reagents.[16,17] In contrast, in the production of plant fiber-based food packaging materials, chemical compounds such as monomers and additives are necessary. Furthermore, modified or bleached plant fibers may pose safety risks due to unclear toxicity mechanisms and toxicological effects.[18] Additionally, the release of microplastics from plastic packaging has raised concerns about human health and safety. Microplastics with small particle sizes can accumulate in various organs and tissues, and may have adverse effects on human health.[19] Therefore, the "edible" nature of the γ-CD-MOF offers a safety advantage, making it a promising material for applications in food packaging.[20,21] Furthermore, polydimethylsiloxane has been used in the packaging field due to its exceptional properties, including excellent thermal stability, biocompatibility, resistance to corrosion, flexibility, low cost, ease of fabrication, and chemical inertness, among others.[22–24]

In this study, a functionalized film was successfully synthesized and characterized in terms of its appearance, thermal stability, and mechanical properties. Subsequently, this film was applied to the preservation of fish meat. The results indicated that the functionalized film exhibited excellent antioxidant and antimicrobial properties. Moreover, compared with a pure film, the functionalized film could reduce the total volatile basic nitrogen (TVB-N), pH, and total viable count (TVC) values of fish meat to a certain extent. As a result, this functionalized film shows great potential for use in fish meat packaging.

2 Materials and methods

2.1 Materials

2,2′-Azino-bis (3-ethylbenzothiazoline-6-sulfonic acid) (98%) and 2,2-diphenyl-1-picrylhydrazyl (98.5%) were purchased from Shanghai Macklin Biochemical Co. Ltd (Shanghai, China). γ-CD (98%) and potassium hydroxide (KOH, 90%) were purchased from Shanghai Macklin Biochemical Co. Ltd (Shanghai, China). Polyethylene glycol 8000 (PEG 8000) was purchased from Shanghai Aladdin Bio-Chem Technology Co. Ltd (Shanghai, China). Methanol (MeOH, 99.5%), acetonitrile (99.5%), chloroauric acid (47.8%) and dichloromethane (99.5%) were obtained from Sinopharm Chemical Reagents Co. Ltd (Shanghai, China). Experimental ultra-pure water was processed by a Smart-N system (Heal Force Biotech, Hk). *Staphylococcus aureus* (ATCC 25923), *Escherichia coli* O157:H7 (ATCC 35150), LB Broth, and LB Nutrient Agar were purchased from Qingdao Hope Bio-technology Co., Ltd (Qingdao, China). Phosphate Buffer Saline (PBS) was purchased from Beijing Solarbio Science & Technology Co., Ltd (Beijing, China). The large yellow croakers used in the experiment were all purchased from a supermarket.

2.2 Preparation of films

The γ-CD-MOF and its complex were synthesized according to the methods outlined in our previous studies.[13] The preparation of the pure film and functionalized films followed the procedure described in our earlier work.[13] More detailed information is listed in SI.

2.3 Characterization of films

A scanning electron microscope (SEM, Gemini SEM 360, ZEISS, Germany) fitted with an energy-dispersive X-ray spectroscopy (EDS) detector was used to investigate the morphological features of the functionalized film. To obtain a smooth, uncontaminated surface for cross-sectional observation, the functionalized film was first frozen and then fractured using liquid nitrogen. Before the SEM measurement, the fractured film samples were attached to conductive adhesive tape and sputter-coated with a thin layer of platinum to improve electrical conductivity.

Powder X-ray diffraction (PXRD) (D8 Advance, Bruker, Germany) was performed on the samples. The experimental conditions were 40 kV tube voltage and 40 mA tube current. All the samples were analyzed over a 2θ angle at a stepwise scan increment of 0.02° with a scanning speed of 0.1 s per step. A Fourier transform infrared spectrometer (FTIR) (Nicolet IS50, Thermo Fisher, USA) was used to collect the spectra of the samples. The samples were thoroughly ground and mixed with potassium bromide before being pressed into a translucent sheet for testing. The wave number range was 500–4000 cm^{-1} with a resolution of 4 cm^{-1}. Additionally, an X-ray photoelectron spectrometer (XPS) (AXIS SUPRA+, Shimadzu, Japan) was employed to characterize the surface elemental composition and chemical environments of the γ-CD-MOF complex.

Thermogravimetric analysis (TGA) was carried out on the functionalized film with a STARe System TGA2 instrument (Mettler Toledo, Switzerland). Approximately 5 mg of the functionalized film sample was used for each TGA test, which was placed in a T_{zero} aluminum crucible. The sample was heated from 25 °C up to 700 °C at a constant heating rate of 10 °C per minute, and a nitrogen flow of 50 mL min^{-1} was kept throughout the process to protect the sample from oxidation. An ultraviolet spectrophotometer (UV-2600, Shimadzu, Japan) was employed to confirm whether γ-CD-MOF complex crystals were present in the functionalized film. The verification process involved two main steps: first, both the γ-CD-MOF complex and the functionalized film were soaked in pure water to prepare solutions with a concentration of 1 mg mL^{-1}. Then, ultraviolet-visible (UV-Vis) absorbance spectra of these two solutions were measured, covering the wavelength range from 300 nm to 700 nm.

2.4 Mechanical properties and water contact angle analysis

A universal testing machine (model Z020, ZwickRoell, Germany) was utilized to assess the mechanical properties of the functionalized film. During the tests, the stretching speed was adjusted to 50 mm per minute, and all measurements were carried out under room temperature conditions. To ensure data reliability, each mechanical test was conducted in triplicate. For the determination of water contact angles, sample discs with a diameter of 1 cm were cut from both the pure film and the functionalized film. To obtain accurate contact angle values, five separate measurements were taken for each film sample, and the results were averaged for subsequent analysis.

2.5 Antioxidant activity

Antioxidant activities of the functionalized films were assessed using $DPPH^{\bullet+}$ and $ABTS^{\bullet+}$ scavenging methods.[25,26] For DPPH analysis, a fresh methanolic solution of DPPH (0.2 mM) was prepared, and 50 mg of the film sample was added to a 10 mL DPPH solution. The mixture was incubated for 30 minutes at room temperature, and then the absorbance was measured at 517 nm. For ABTS analysis, potassium sulfate (2.45 mM) was mixed with ABTS solution (7 mM) in equal volumes and incubated for 12–16 hours in the dark to prepare the ABTS assay solution. Then, 500 mg of film sample was added to 10 mL of the ABTS assay solution, and the mixture was incubated at room temperature for 30 minutes in the dark. The absorbance was then measured at 734 nm. The antioxidant activity of all the films was determined as follows:

$$\text{Free radicalscavenging activity}(\%) = \frac{A_c - A_s}{A_c} \times \%$$

where A_c and A_s represent the absorbance of DPPH and ABTS for the control and film samples, respectively. The test was repeated in triplicate.

2.6 Antibacterial activity

To assess the films' antibacterial activity, two model bacterial strains were selected: *S. aureus* and *E. coli* O157:H7. First, these bacterial strains were grown in LB medium. The culture was maintained at 37 °C with constant shaking at 180 rpm for a 17-hour period. Using the plate count technique, the bacterial suspension was diluted with sterile PBS to a final concentration of 1×10^6 CFU mL^{-1}. Next, 100 μL of this standardized bacterial solution was pipetted onto the surface of two types of films: pure films and functionalized films. Each film had a diameter of 18 mm. To ensure thorough contact between the bacterial solution and the film surface, a second film was placed on top of the bacterial suspension, creating a sandwich-like structure. These film–bacteria assemblies were then incubated at 37 °C for 24 hours. Post-incubation, 4900 μL of PBS was added to the system to rinse the films and dilute any remaining bacterial solution. The number of viable bacterial colonies was subsequently quantified using the plate count method once more. Additionally, a transmission electron microscope (TEM) (JEM-1230 TEM, HITACHI, Japan) was used to examine the morphological changes in the bacterial cells.

2.7 Antibacterial mechanism

Cell membrane integrity was evaluated by quantifying the leakage of nucleic acids and proteins into the bacterial suspension. This quantification was performed using an ultraviolet-visible spectrophotometer (Model: NanoDrop One/One C, Manufacturer: Thermo Scientific, U.S.A.). Specifically, nucleic acid concentration was determined by measuring the optical density (OD) at a wavelength of 260 nm, while protein concentration was assessed *via* OD measurement at 280 nm, in accordance with previously established protocols.[27–29] For sample preparation, bacterial solutions exposed to functionalized films for different time intervals were subjected to centrifugation. The centrifugation process was conducted at 8000 rpm for 10 minutes at a temperature of 25 °C. Following centrifugation, the supernatant was collected to determine the absorbance values at 260 nm and 280 nm. Separately, the mitochondrial membrane potential of bacteria was evaluated using the Rhodamine 123 (Rh 123) fluorescent staining assay.[30,31] Bacterial solutions after treatment were first centrifuged at 25 °C, 8000 rpm for 10 minutes. The resulting bacterial pellet was then washed three times with PBS. After washing, the bacteria were resuspended in 1 mL of Rh 123 solution (with a final concentration of 2 μg mL^{-1}) and incubated in the dark at room temperature for 30 minutes. Post-incubation, the bacterial samples were washed twice with PBS to eliminate unbound Rh 123. The fluorescence spectra of the samples were subsequently measured using a multimode microplate reader. The detection parameters were set as follows: excitation wavelength at 480 nm, emission wavelength at 530 nm, and a gain value of 80.

2.8 Freshness of large yellow croakers during storage

2.8.1 pH analysis. The pH test was conducted using a method previously reported with minor modifications.[32] 1 g of fish muscle sample was treated with pure and functionalized films for different durations. The fish was then chopped and placed into centrifuge tubes. Following this, the chopped fish

was mixed with 6 mL of distilled water, and the pH of the mixture was measured using a pH meter (PHS-25, Shanghai INESA Scientific Instrument Co., Ltd, China).

2.8.2 TVB-N analysis. The TVB-N content is a critical indicator of meat freshness. TVB-N was analyzed using the micro-diffusion method, according to the GB5009.228-2016 standard.

2.8.3 TVC analysis. Microbial analysis was performed following a previously reported method with slight modifications.[33] Specifically, after treatment with pure and functionalized films, 1 g of chopped fish was placed into a sterile centrifuge tube containing 9 mL of physiological saline solution. The mixture was thoroughly homogenized, and serial dilutions were carried out. Three appropriate dilutions were selected for further analysis. The plate counting method was then used to quantify the bacterial colonies, with the results expressed in log CFU g^{-1}.

2.9 Statistical analysis

All data were analyzed using analysis of variance (ANOVA) in IBM SPSS Statistics 25.0. When the overall P value for the experiment was below the significance threshold ($P < 0.05$), Tukey's test was used to compare the means. Graphs were generated using Origin 2018 and GraphPad Prism 9, based on data from three independent replicate experiments.

3 Results and discussion

3.1 Characterization of films

Scheme 1 presents the preparation process and application of the functionalized film. As exhibited in Fig. 1a, the SEM image of the functionalized film surface displays a large number of cubic crystals corresponding to the γ-CD-MOF complex. Fig. 1b demonstrates partial integration of the γ-CD-MOF complex crystals into the matrix of the functionalized film. In contrast, Fig. 1c and d provide the surface and cross-sectional SEM images of the pure film, respectively, with no embedded crystals observed in either case.

Fig. 1e presents the PXRD patterns of different samples. As shown in the figure, the γ-CD-MOF complex exhibits distinct and intense characteristic diffraction peaks, whereas the pure

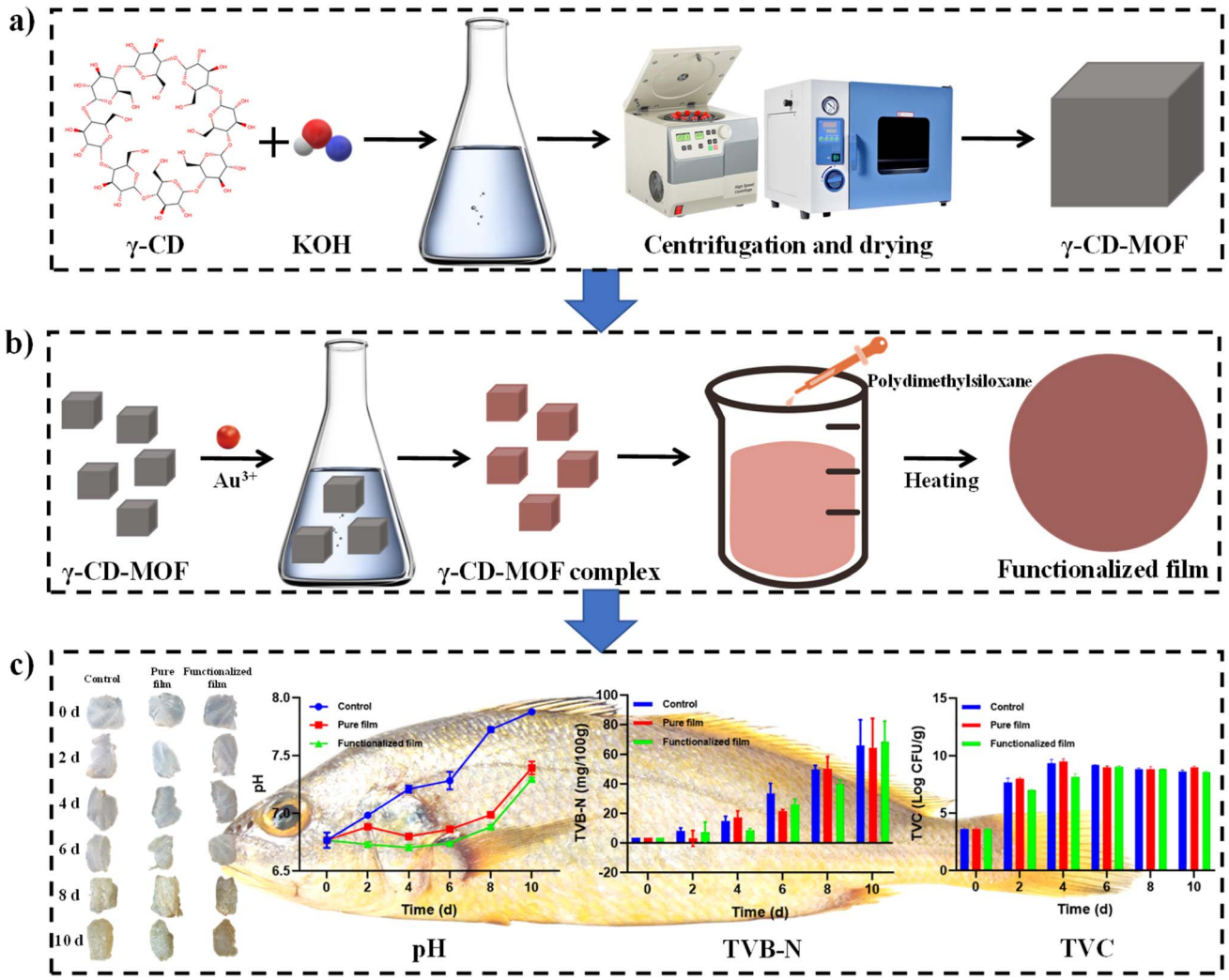

Scheme 1 Schematic of preparation of the (a) γ-CD-MOF, (b) γ-CD-MOF complex and functionalized film, and (c) the application of the functionalized film in preserving the freshness of large yellow croakers.

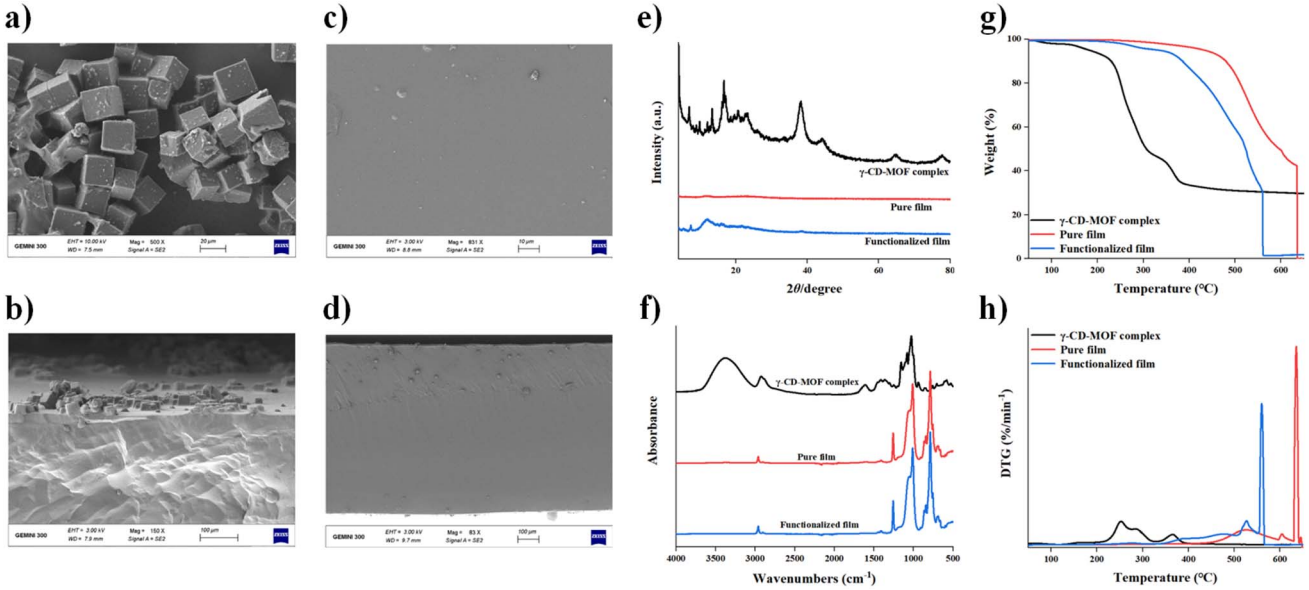

Fig. 1 (a) Surface and (b) cross-section SEM images of the functionalized film; (c) surface and (d) cross-section SEM images of the pure film; (e) PXRD patterns, (f) FTIR spectra, (g) TGA and (h) DTG spectra of the γ-CD-MOF complex, pure film, and functionalized film.

film and functionalized film display extremely weak characteristic peaks without the emergence of new diffraction peaks. This indicates that the incorporation of the γ-CD-MOF complex into the film is likely mediated by physical interactions. To further verify the interaction between the γ-CD-MOF complex and the functionalized film, FTIR was performed on the samples (Fig. 1f). The results reveal that the FTIR spectrum of the functionalized film is almost identical to that of the pure film, with no new absorption bands formed. This confirms that the interaction between the γ-CD-MOF complex and the functionalized film is of a physical nature.

The effect of partially embedded γ-CD-MOF complex crystals on the thermal stability of the functionalized film is illustrated in Fig. 1g and h. A prominent weight loss of the γ-CD-MOF complex is observed in the temperature range of 250–380 °C, which is attributed to the thermal degradation of the cyclodextrin component and the full decomposition of the γ-CD-MOF structure.[34,35] For the pure film, a 50% weight loss is achieved at 595 °C, which aligns with findings reported in previous literature.[36] By comparison, the functionalized film exhibits a 50% weight loss at 520 °C, a temperature notably lower than that of the pure film. These results indicate that the incorporation of γ-CD-MOF complex crystals impairs the thermal stability of the functionalized film. While the incorporation of the γ-CD-MOF complex moderately compromises the thermal stability of the functionalized film, the film still retains satisfactory thermal stability. As illustrated in Fig. 1g, the functionalized film exhibits negligible weight loss until the heating temperature exceeds 300 °C. Notably, the temperature employed in traditional thermal processing of foodstuffs generally does not exceed 250 °C.[37] Furthermore, to pursue healthier and more nutritious food products, non-thermal processing technologies have been increasingly adopted in recent years.[38]

Fig. 2a shows the UV-Vis absorption peaks of the γ-CD-MOF complex and the functionalized film after immersion in water, with these peaks being ascribed to gold nanoparticles.[39] This observation confirms the successful incorporation of γ-CD-MOF complex crystals into the functionalized film. To further verify the formation of gold nanoparticles, XPS analysis was performed on the γ-CD-MOF complex. The results revealed characteristic peaks at 87.8 eV and 84.1 eV, which are attributed to Au $4f_{5/2}$ and Au $4f_{7/2}$, respectively (Fig. S1). These findings confirm the successful formation of gold nanoparticles. Additionally, the gold content in the γ-CD-MOF complex was determined, with a loading efficiency of approximately 2.2% (Fig. S2). In Fig. 2b, the potassium signal verifies the presence of the γ-CD-MOF, while the gold signal confirms the existence of gold nanoparticles again. Furthermore, Fig. 2b reveals that γ-CD-MOF complex crystals are uniformly distributed on the surface of the functionalized film.[40] Finally, the cytotoxicity of the γ-CD-MOF complex was investigated, and the results demonstrated that it exhibits no cytotoxicity within the concentration range of 62.5–1000 μg mL^{-1} (Fig. S3).

3.2 Mechanical properties and water contact analysis

Mechanical properties are of critical importance to food packaging films during the packaging process, thereby highlighting the necessity of guaranteeing their superior performance.[41,42] As presented in Fig. 3a, the stress–strain curve of the functionalized film is analogous to that of the pure film, which implies that the two films possess comparable elastic behaviors. Fig. 3b demonstrates that the tensile strength of the functionalized film is on par with that of the pure film. Furthermore, the incorporation of γ-CD-MOF complex crystals remarkably improves the elastic modulus of the functionalized film, while simultaneously reducing its elongation at break, as evidenced in Fig. 3c and d.

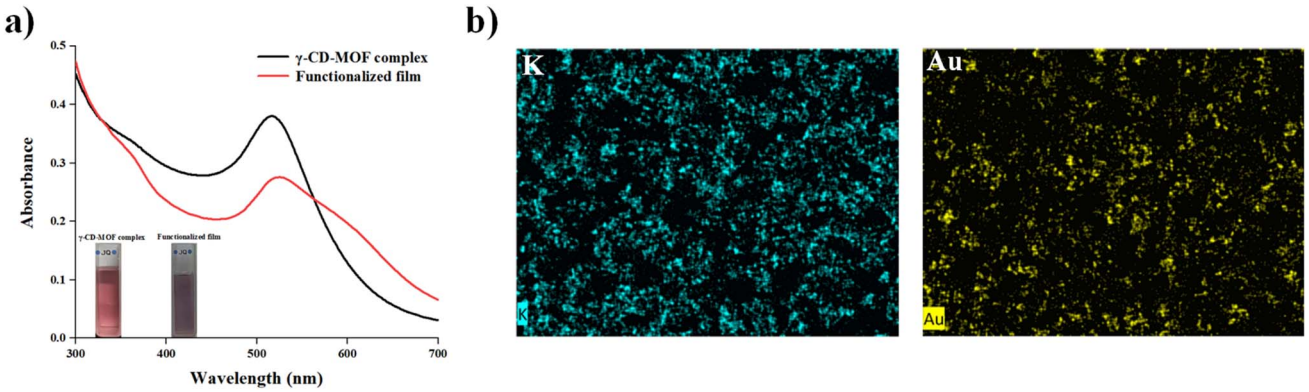

Fig. 2 (a) UV-Vis absorbance spectra of the γ-CD-MOF complex and functionalized film immersed in water; (b) EDS elemental mapping of the functionalized film (K signal: blue; Au signal: yellow).

Hydrophilic food packaging materials are prone to being affected by humid environments, which severely restricts their application in the preservation and transportation of food products. Consequently, improving the water resistance of these packaging materials is of great significance.[43] To assess the hydrophobic properties of the films, water contact angle analysis was conducted. As shown in Fig. 3e, the functionalized film exhibits hydrophobic characteristics, though its water contact angle is notably lower than that of the pure film. This phenomenon can be ascribed to the high hydrophilicity of the γ-CD-MOF, whose structure contains a large number of hydrophilic hydroxyl groups.[20] Despite the inherent hydrophobicity of polydimethylsiloxane, the introduction of γ-CD-MOF complex crystals leads to a reduction in its water contact angle. Additionally, a comparison of the WVTR between the pure film and the functionalized film was conducted (Fig. S4). The results demonstrate that under identical conditions, the WVTR values of the pure film and the functionalized film are 150.68 and

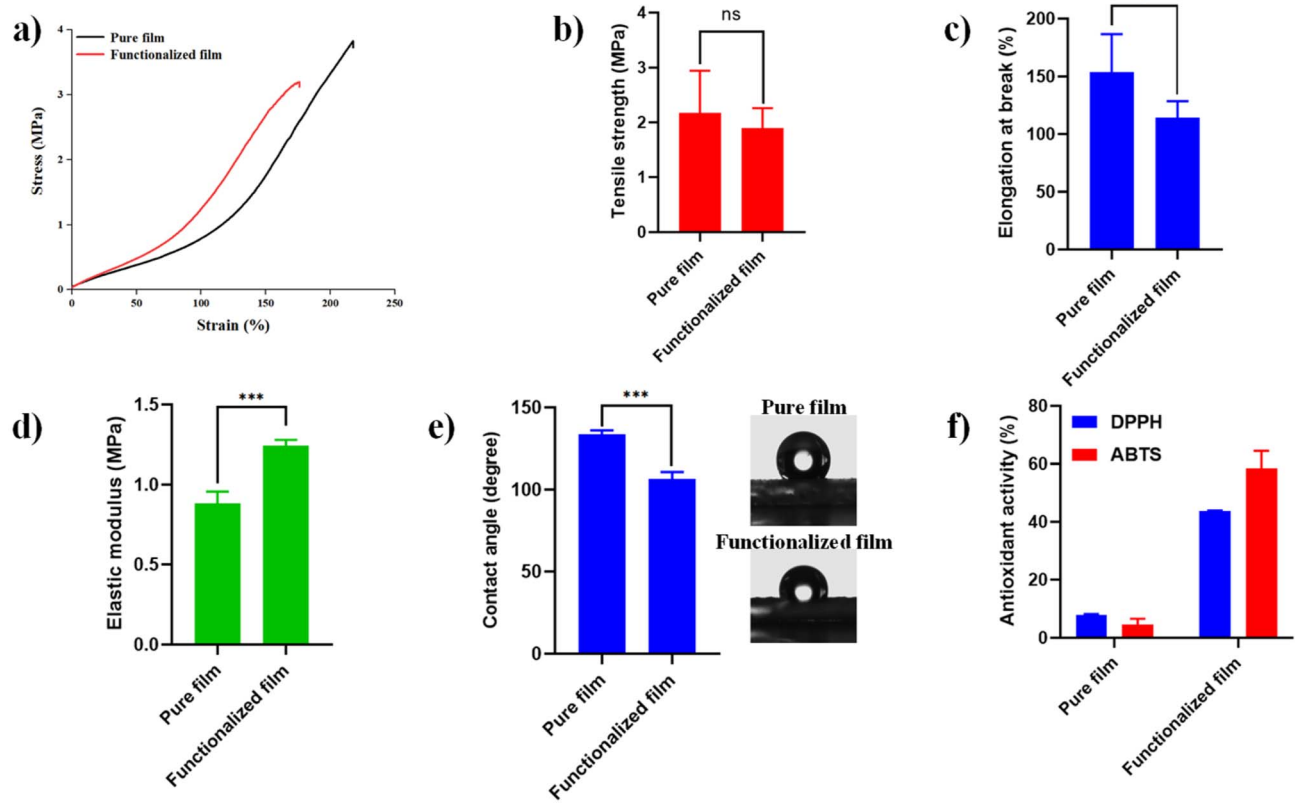

Fig. 3 Mechanical properties of the pure film and functionalized film, including (a) stress–strain curves, (b) tensile strength, (c) elongation at break, and (d) elastic modulus. (e) Contact angle and (f) antioxidant activity of the pure film and functionalized film.

173.37 (g (m^2 24 h)$^{-1}$), respectively. This observation indicates that the incorporation of the γ-CD-MOF complex moderately enhances the WVTR of the functionalized film.

3.3 Antioxidant properties

The antioxidant activity and free radical scavenging ability of food packaging films are critical, as free radicals can cause food discoloration, rancidity, and off-flavors.[44] The antioxidant activity of the films was evaluated based on ABTS and DPPH free radical scavenging assays, with the results presented in Fig. 3f. The functionalized film showed 44% DPPH scavenging activity and 58% ABTS scavenging activity. Although the DPPH and ABTS free radical scavenging capacities of the functionalized film were lower than those of organoselenocyanate-tethered methyl anthranilate hybrids and organodiselenide-tethered methyl anthranilates,[45,46] they were significantly higher than those of the pure film, as the latter exhibited only about 8% DPPH scavenging activity and 5% ABTS scavenging activity. The antioxidant activity of the functionalized film is attributed to the released gold nanoparticles, which exhibit significant antioxidant properties due to the unique characteristics of their nanoparticle surfaces.[47,48] Furthermore, the free radical scavenging activity of the functionalized film, as measured by the ABTS assay, was slightly higher than that observed with the DPPH assay. This can be explained by the greater solubility of the γ-CD-MOF in pure water, which facilitates enhanced release of gold nanoparticles.[44]

3.4 Antibacterial properties

To evaluate the antibacterial effectiveness of the films, both *E. coli* O157:H7 and *S. aureus* were used as test microorganisms. The antibacterial performance against *E. coli* O157:H7 is shown

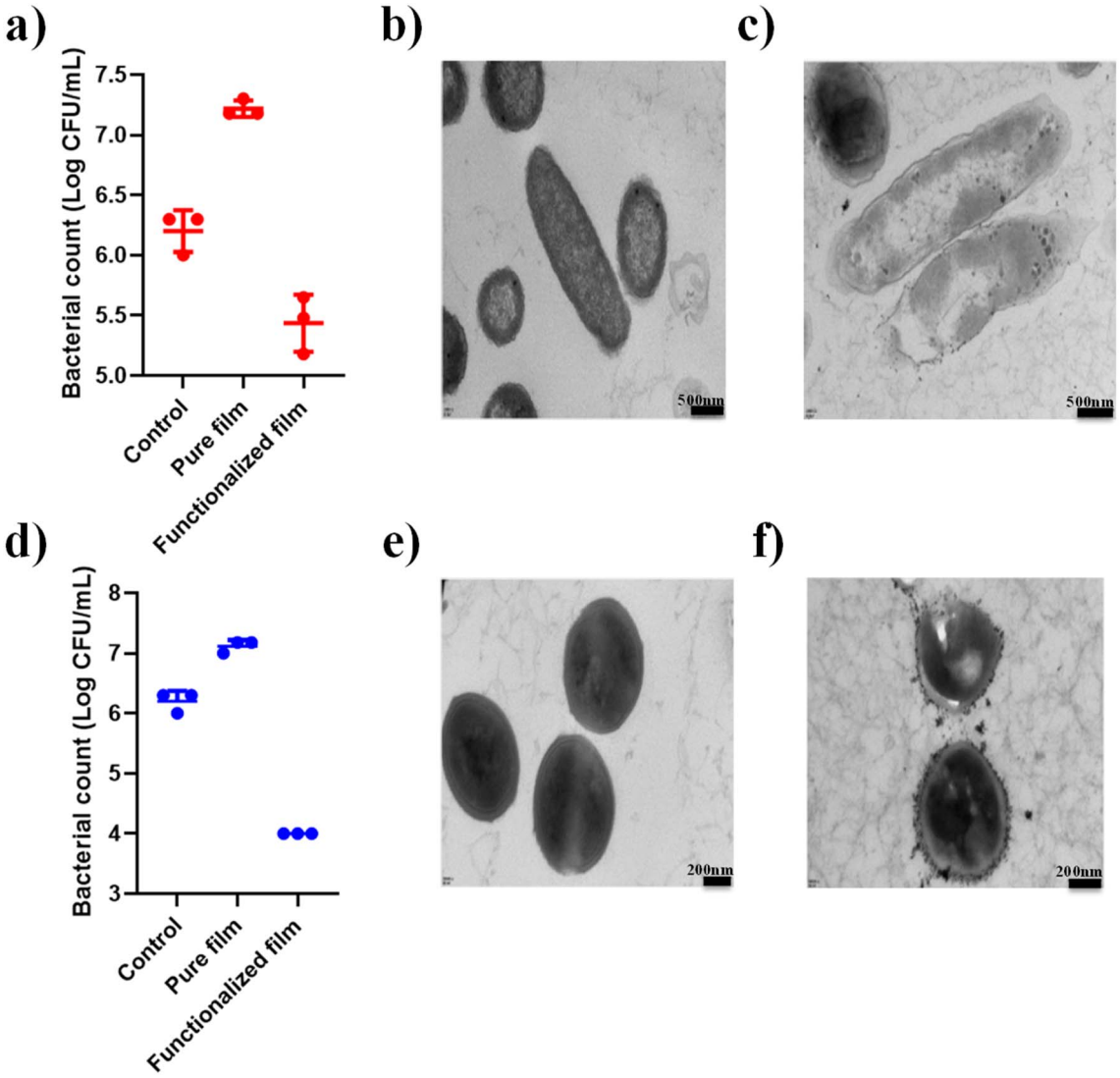

Fig. 4 Antibacterial activity of the pure film and functionalized film against (a) *E. coli* O157:H7 and (d) *S. aureus*; TEM images of *E. coli* O157:H7 as (b) a control and (c) after 24 hours treatment with the functionalized film; TEM images of *S. aureus* as (e) a control and (f) after 24 hours treatment with the functionalized film.

in Fig. 4a. In comparison to the control, the bacterial population on the pure film increased after 24 hours, indicating that *E. coli* O157:H7 adhered to the pure film surface, promoting bacterial growth.[49] This suggests that the pure film does not effectively inactivate *E. coli* O157:H7. In contrast, after 24 hours of exposure to the functionalized film, a significant reduction in bacterial count was observed, highlighting the functionalized film's strong antibacterial properties against *E. coli* O157:H7. Similarly, Fig. 4d further demonstrates that the functionalized film also significantly reduced the bacterial counts of *S. aureus*. Taken together, these findings indicate that the functionalized film exhibits potent antibacterial activity, likely due to the release of gold nanoparticles, which are known to have intrinsic antibacterial properties.[13]

TEM images in Fig. 4b and c illustrate the morphology of untreated and treated *E. coli* O157:H7, respectively. As shown in Fig. 4b, the control *E. coli* O157:H7 retains an intact cell membrane and characteristic structure. In contrast, after exposure to the functionalized film, *E. coli* O157:H7 exhibits severe damage, including cell lysis, membrane disruption, and abnormal cellular swelling (Fig. 4c).[50] Analogously, Fig. 4e and f demonstrate that control *S. aureus* has intact membranes, while treated *S. aureus* shows extensive damage. A large number of gold nanoparticles are observed adhering to *S. aureus* cell surfaces, resulting in membrane rupture and leakage of intracellular contents.[50,51] Additionally, the gold nanoparticles may interact with other organelles such as the cell membrane and may also inhibit specific proteins involved in cellular respiration, thus causing cell death.[52–54]

3.5 Antibacterial mechanism

In bacteria, the cell membrane functions as a protective barrier. Disruption of the cell membrane by antimicrobial agents leads to the leakage of intracellular ions (*e.g.*, K^+ and Na^+) and other macromolecules.[28] Additionally, macromolecules such as nucleic acids and proteins exhibit characteristic absorbance peaks at 260 nm and 280 nm, respectively.[55] Fig. 5a and b depict the leakage of nucleic acids and proteins from *E. coli* O157:H7, while Fig. 5d and e show the same for *S. aureus*. The results reveal that the absorbance values of all experimental groups are significantly higher than those of the control groups. This confirms that treatment with the functionalized film caused severe disruption, thereby impairing the integrity and permeability of the bacterial cell membrane.[28,56]

Rh 123, a positively charged probe that enters cells through diffusion, was employed to assess the mitochondrial membrane potential.[57] Under normal circumstances, cells sustain stable intracellular membrane potentials, which are crucial for maintaining normal cellular function.[58] The results of the membrane potential assays for *E. coli* O157:H7 and *S. aureus* are presented in Fig. 5c and f, respectively. These results show that the mitochondrial membrane potential in the control groups was higher than that in the experimental groups. Furthermore, the fluorescence intensities of both control and experimental groups decreased steadily over time. This implies that an increasing proportion of bacteria might have entered an inactive state with prolonged incubation.[59,60] Taken together, these findings confirm that treatment with the functionalized film induced a reduction in the mitochondrial membrane potential of the tested bacteria.

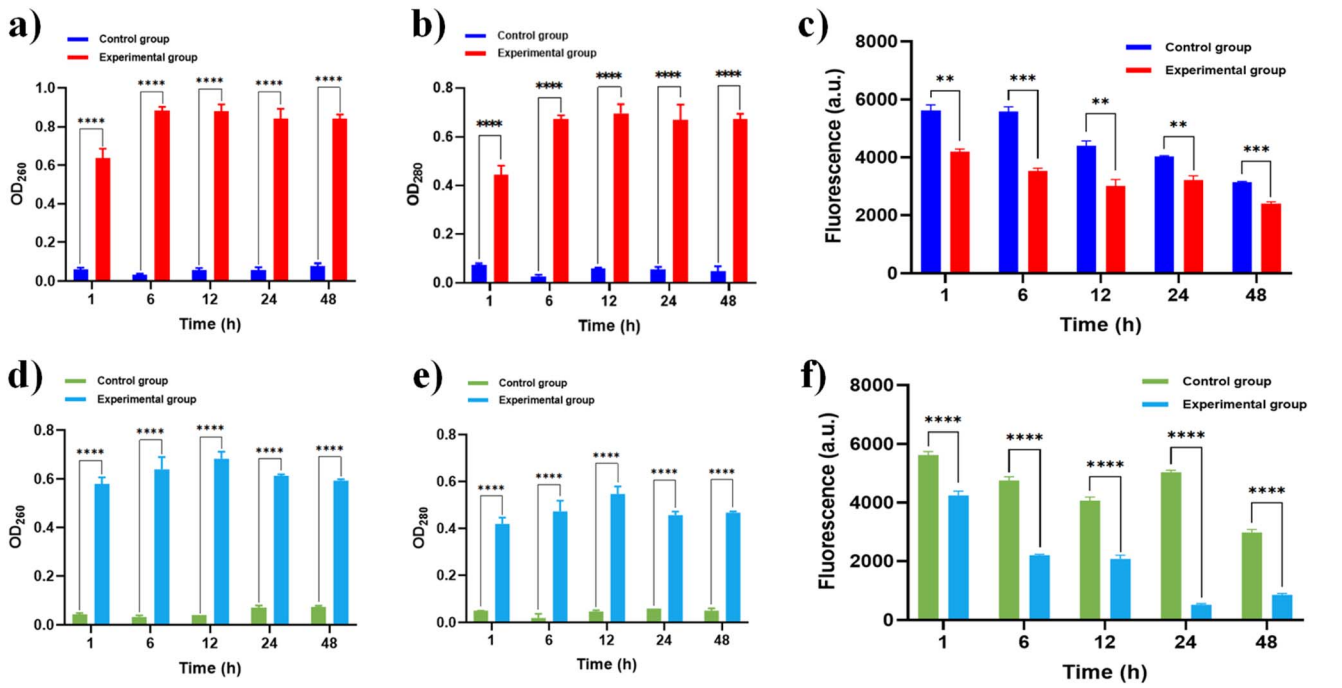

Fig. 5 Changes in (a) nucleic acids, (b) proteins, and (c) membrane potential of *E. coli* O157:H7 after treatment with the functionalized film for different times. Changes in (d) nucleic acids, (e) proteins, and (f) membrane potential of *S. aureus* after treatment with the functionalized film for different times.

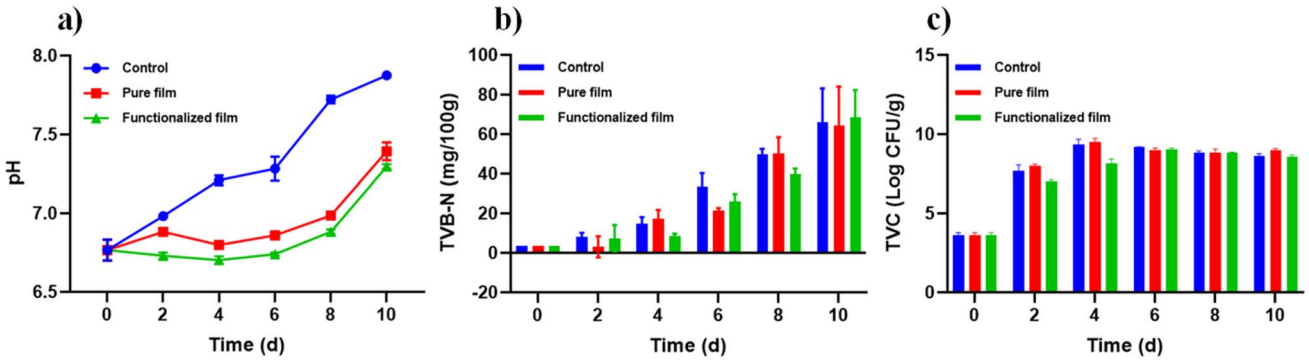

Fig. 6 Effects of the pure film and functionalized film on various parameters, including (a) pH, (b) TVB-N, and (c) TVC of fish fillets stored under controlled conditions at 4 °C.

3.6 Freshness of large yellow croakers during storage

3.6.1 pH analysis. pH is a crucial indicator for evaluating the quality of fish products. The trend of pH changes in fish fillets during storage at 4 °C is shown in Fig. 6a. It clearly illustrates that pH increased over the storage period, with values rising from the beginning to the 10th day. The pH of the control group rapidly increased to 7.8 by the 10th day. In contrast, the pH of the pure film and functionalized film groups increased more gradually during the first 6 days. Specifically, in the functionalized film group, the pH of the fish fillets started at 6.76 ± 0.07 on day 1, dropped slightly to 6.70 ± 0.02 on day 4, and then steadily increased to 7.29 ± 0.02 by day 10. Similar results were reported in previous studies.[61]

The primary cause of the initial pH decline is the hydrolysis of ATP to phosphoric acid following the death of the fish, along with the anaerobic degradation of glycogen to lactic acid. This process leads to the accumulation of acidic metabolites, resulting in a decrease in pH.[62] In the later stages, as the fish enters the autolytic spoilage phase, proteolytic enzymes and alkaline microorganisms break down proteins into volatile compounds such as ammonia, dimethylamine, and trimethylamine. This process leads to an increase in pH due to the accumulation of these alkaline substances.[63]

3.6.2 TVB-N analysis. TVB-N levels are a critical indicator of nitrogenous compounds, particularly volatile amines, produced during the breakdown of proteins in fish meat.[64] Fig. 6b presents the TVB-N test results for fish stored at 4 °C. The TVB-N value increased with storage time across all groups. However, the functionalized film group consistently exhibited lower values compared to both the pure film and control groups. For instance, on day 4, the TVB-N value for the functionalized film was only 8.71 mg/100 g, whereas the pure film and the control group had values of 17.42 mg/100 g and 14.93 mg/100 g, respectively. Moreover, during the first six days, the functionalized film maintained a relatively low TVB-N value of approximately 26.13 mg/100 g. A similar result was reported in a previous study.[65] Proteins in fresh meat decompose, leading to the production of TVB-N, which primarily consists of ammonia compounds and dimethylamine. This process occurs due to the interaction between proteases produced by microbial metabolism and endogenous enzymes in fresh meat.[66] Therefore, the lower TVB-N value in the functionalized film group is likely due to more microorganisms being inactivated, resulting in less protease production as a result of the antibacterial properties of gold nanoparticles in the functionalized film.[67] According to the Chinese Standard GB 2707-2016, the TVB-N limit for edible fish is set at 30 mg/100 g, and fish with TVB-N levels above this threshold are considered spoiled. Therefore, these results suggest that the functionalized film performed effectively in maintaining fish freshness.

3.6.3 TVC analysis. The surface of a dead fish harbors numerous bacteria, which accelerate the decay process. Therefore, the measurement of the TVC is one of the most critical criteria for evaluating the quality of stored fish.[68] Fig. 6c presents the TVC results for fish stored at 4 °C from day 0 to day 10. On day 1, the fish's bacterial count in all groups was only 3.61 ± 0.17 log CFU g^{-1}. However, the bacterial count increased rapidly as storage time progressed, likely due to the fish providing an ideal environment for bacterial growth.[69] The functionalized film group exhibited a lower bacterial count compared to both the control and pure film groups during the first four days. This slower increase in bacterial count can be attributed to the strong antibacterial properties of the γ-CD-MOF complex in the functionalized film, which helps prevent microbial growth. These results demonstrate that the functionalized film possesses effective antibacterial and preservative capabilities. Finally, the stability of the functionalized film was indirectly evaluated by testing the UV-Vis spectra of the γ-CD-MOF complex stored at different temperatures for 7 days (Fig. S5). The results showed that the UV-Vis spectra were almost identical across all tested temperatures, indicating that the functionalized film can exist stably and maintain its continuous functionality.

4 Conclusion

In this study, a functionalized film was successfully fabricated by immobilizing a γ-CD-MOF complex onto a polydimethylsiloxane substrate. Characterization revealed that the γ-CD-MOF complex modulated the film's physicochemical properties, including the tensile strength and water contact

angle, which are key parameters for packaging applicability. The film exhibited remarkable antioxidant activity with $DPPH^{\bullet+}$ and $ABTS^{\bullet+}$ scavenging rates of 44% and 58%, respectively, significantly higher than those of the pure PDMS film, as well as potent antibacterial efficacy that reduced *E. coli* O157:H7 by 99.4% and *S. aureus* by 80% within 24 hours. During 4-day refrigerated storage of fish fillets, it effectively maintained pH at 6.70 ± 0.02 and TVB-N at 8.71 mg/100 g while suppressing TVC to levels substantially lower than those in the control and pure film groups. Collectively, the functionalized film prolongs the shelf life of refrigerated fish fillets by inhibiting microbial proliferation and retarding lipid oxidation, ensuring storage safety and freshness. Future work will focus on expanding applicability to more aquatic products, and investigating biodegradability to align with green packaging trends, thereby promoting its practical use in food preservation and packaging.

Author contributions

Meimei Guo: writing – review & editing, writing – original draft, software, methodology, investigation, formal analysis, data curation. Tahirou Sogore: writing – review & editing, formal analysis. Jin Huang: writing – review & editing, formal analysis. Xinyu liao: writing – review & editing, formal analysis. Mofei Shen: writing – review & editing, formal analysis. Tian Ding: writing – review & editing, validation, supervision, conceptualization, funding acquisition.

Conflicts of interest

The authors declare that they have no known competing financial interests or personal relationships that could have appeared to influence the work reported in this paper.

Data availability

The data supporting the findings of this study and supplementary information are available from the corresponding author upon reasonable request.

Supplementary information (SI): Fig. S1 shows the high-resolution Au 4f XPS spectra obtained from the γ-CD-MOF complex; Fig. S2 shows the gold ion loading rate of the γ-CD-MOF complex; Fig. S3 shows the *in vitro* cell viability of Caco-2 cells exposed to the γ-CD-MOF complex; Fig. S4 shows the water vapor transmittance rate of pure films and functionalized films; Fig. S5 shows the UV-Vis absorbance spectra of the γ-CD-MOF complex stored at different temperatures for 7 days. See DOI: https://doi.org/10.1039/d5fb00743g.

Acknowledgements

This work was supported by the National Key Research and Development Program of China (2022YFF1102700), and the Starry Night Science Fund of Zhejiang University Shanghai Institute for Advanced Study (Grant No. SN-ZJU-SIAS-004).

References

1 J. M. Lorenzo, R. Batlle and M. Gómez, Extension of the shelf-life of foal meat with two antioxidant active packaging systems, *LWT–Food Sci. Technol.*, 2014, **59**, 181–188.
2 R. Eshaghi, M. Mohsenzadeh and J. F. Ayala-Zavala, Bio-nanocomposite active packaging films based on carboxymethyl cellulose, myrrh gum, TiO_2 nanoparticles and dill essential oil for preserving fresh-fish (Cyprinus carpio) meat quality, *Int. J. Biol. Macromol.*, 2024, **263**, 129991.
3 J. Tavares, A. Martins, L. G. Fidalgo, V. Lima, R. A. Amaral, C. A. Pinto, A. M. Silva and J. A. Saraiva, Fresh Fish Degradation and Advances in Preservation Using Physical Emerging Technologies, *Foods*, 2021, **10**, 10040780.
4 M. N. Madhubhashini, C. P. Liyanage, A. U. Alahakoon and R. P. Liyanage, Current applications and future trends of artificial senses in fish freshness determination: A review, *J. Food Sci.*, 2024, **89**, 33–50.
5 E. Sánchez-López, D. Gomes, G. Esteruelas, L. Bonilla, A. L. Lopez-Machado, R. Galindo, A. Cano, M. Espina, M. Ettcheto, A. Camins, M. S. Amélia, D. Alessandra, S. Antonello, L. G. Maria and B. S. Eliana, Metal-Based Nanoparticles as Antimicrobial Agents: An Overview, *Nanomaterials*, 2020, **10**(2), 292.
6 A. Evans and A. K. Kevin, Evaluation of metal-based antimicrobial compounds for the treatment of bacterial pathogens, *J. Med. Microbiol.*, 2021, **70**(5), 001363.
7 X. Xie, J. Tian, J. Wu, R. Guo, J. Zhang, D. Fu, H. Wang, B. Niu and H. Yan, Polylactic Acid/Poly(Butylene Adipate-Co-Terephthalate) Packing Films Doped with Novel Antimicrobial Agent CuO@γ-CD-MOFs, *ChemistrySelect*, 2025, **10**, e02743.
8 S. Kumari, A. Kumari and R. Sharma, Safe and sustainable food packaging: Argemone albiflora mediated green synthesized silver-carrageenan nanocomposite films, *Int. J. Biol. Macromol.*, 2024, **264**, 130626.
9 A. M. Pak, E. N. Zakharchenko, E. A. Maiorova and V. V. Novikov, Bicompatible Metal-Organic Framework for Functional Packing of Food Products, *Russ. J. Coord. Chem.*, 2023, **49**, 97–103.
10 M. Sriubas, K. Bockute, P. Palevicius, M. Kaminskas, Z. Rinkevicius, M. Ragulskis, S. Simonyte, M. Ruzauskas and G. Laukaitis, Antibacterial Activity of Silver and Gold Particles Formed on Titania Thin Films, *Nanomaterials*, 2022, **12**(7), 1190.
11 D. Mitra, E. T. Kang and K. G. Neoh, Antimicrobial Copper-Based Materials and Coatings: Potential Multifaceted Biomedical Applications, *ACS Appl. Mater. Interfaces*, 2020, **12**(19), 21159–21182.
12 E. M. Cazalini, W. Miyakawa, G. R. Teodoro, A. S. S. Sobrinho, J. E. Matieli, M. Massi and C. Y. Koga-Ito, Antimicrobial and anti-biofilm properties of polypropylene meshes coated with metal-containing DLC thin films, *J. Mater. Sci. Mater. Med.*, 2017, **28**(6), 97.

13 M. Guo, M. Shen, Y. Zhu, T. Sogore and T. Ding, Ultra-small gold nanoparticles embedded cyclodextrin metal-organic framework composite membrane to achieve antibacterial and humidity-responsive functions, *Carbohydr. Polym.*, 2024, **340**, 122200.
14 J. Jeevanandam, S. F. Kiew, S. Boakye-Ansah, S. Y. Lau, A. Barhoum, M. K. Danquah and J. Rodrigues, Green approaches for the synthesis of metal and metal oxide nanoparticles using microbial and plant extracts, *Nanoscale*, 2022, **14**, 2534–2571.
15 B. A. Suliasih, S. Budi and H. Katas, Synthesis and application of gold nanoparticles as antioxidants, *Pharmacia*, 2024, **71**, 1–19.
16 I. Roy and J. F. Stoddart, Cyclodextrin Metal-Organic Frameworks and Their Applications, *Acc. Chem. Res.*, 2021, **54**(6), 1440–1453.
17 A. Hamedi, A. Anceschi, A. Patrucco and M. Hasanzadeh, A γ-cyclodextrin-based metal-organic framework (γ-CD-MOF): a review of recent advances for drug delivery application, *J. Drug Targeting*, 2021, **30**(4), 381–393.
18 M. Tang, C. Chen, J. Song, Y. Ni, B. Xiang, J. Zou and D. Xu, Safety of plant fiber-based food contact materials: Overview of the discovery, identification, detection and risk assessment of unknown risk substances, *Food Packag. Shelf Life*, 2024, **43**, 101281.
19 J. Čurlej, P. Zajác, J. Čapla and L. Hleba, Safety issues of microplastics released from food contact materials, *J. Microbiol. Biotechnol. Food Sci.*, 2023, **13**(2), e10317.
20 R. A. Smaldone, R. S. Forgan, H. Furukawa, J. J. Gassensmith, A. M. Z. Slawin, O. M. Yaghi and J. . F. Stoddart, Metal-Organic Frameworks from Edible Natural Products, *Angew. Chem., Int. Ed.*, 2010, **49**, 8630–8634.
21 S. Li, X. Hu, S. Chen, X. Wang, H. Shang, Y. Zhou, J. Dai, L. Xiao, W. Qin and Y. Liu, Synthesis of γ-cyclodextrin metal-organic framework as ethylene absorber for improving postharvest quality of kiwi fruit, *Food Hydrocoll.*, 2023, **136**, 108294.
22 R. Ariati, F. Sales, A. Souza, R. A. Lima and J. Ribeiro, Polydimethylsiloxane Composites Characterization and Its Applications: A Review, *Polymers*, 2020, **13**(23), 4258.
23 Y. Song, S. Sun, Q. Hao, S. Gao, W. Wang and H. Hou, Effect of polydimethylsiloxane on the structure and barrier properties of starch/PBAT composite films, *Carbohydr. Polym.*, 2024, **336**, 122119.
24 F. Wang, L. Qiu and Y. Tian, Super Anti-Wetting Colorimetric Starch-Based Film Modified with Poly(dimethylsiloxane) and Micro-/Nano-Starch for Aquatic-Product Freshness Monitoring, *Biomacromolecules*, 2021, **22**, 3769–3779.
25 S. Roy, R. Priyadarshi and J. Rhim, Gelatin/agar-based multifunctional film integrated with copper-doped zinc oxide nanoparticles and clove essential oil Pickering emulsion for enhancing the shelf life of pork meat, *Food Res. Int.*, 2022, **160**, 111690.
26 S. Roy and J. Rhim, Gelatin/agar-based functional film integrated with Pickering emulsion of clove essential oil stabilized with nanocellulose for active packaging applications, *Colloids Surf., A*, 2021, **627**, 127220.
27 B. Zhang, Y. Zang, Q. Mo, L. Sun, M. Tu, D. Shu, Y. Li, F. Xue, G. Wu and X. Zhao, Antibacterial activity and mechanism of slightly acidic electrolyzed water (SAEW) combined with ultraviolet light against Staphylococcus aureus, *LWT*, 2023, **182**, 114746.
28 H. Gao, M. Sun, Y. Duan, Y. Cai, H. Dai and T. Xu, Controllable synthesis of lignin nanoparticles with antibacterial activity and analysis of its antibacterial mechanism, *Int. J. Biol. Macromol.*, 2023, **246**, 125596.
29 L. Dou, R. Xue, W. Deng, J. Wang, X. Liao, R. Yu, X. Duan and Y. Xiong, Design, synthesis and evaluation of phenyl sulfonyl fluoride substituted ruthenium polypyridine complex as antibacterial agent targeting cell membrane, *J. Mol. Struct.*, 2025, **1319**, 139591.
30 J. Comas and J. Vives-Rego, Assessment of the effects of gramicidin, formaldehyde, and surfactants on Escherichia coli by flow cytometry using nucleic acid and film potential dyes, *Cytometry*, 1997, **29**, 58–64.
31 Y. Zhang, X. Liu, Y. Wang, P. Jiang and S. Quek, Antibacterial activity and mechanism of cinnamon essential oil against Escherichia coli and Staphylococcus aureus, *Food Control*, 2015, **59**, 282–289.
32 X. Fan, L. Yin, J. Zhu, P. Sun, Y. Zhu, Q. Chen, B. Kong, Q. Liu and H. Wang, The improvement of storage quality of Harbin red sausage by coating with oregano essential oil loaded zein-pectin-chitosan nanoparticles, *Food Packag. Shelf Life*, 2024, **43**, 101274.
33 A. Lv, G. Fan, Z. Yang, Z. Zhang, M. M. Khan and X. Fu, Polydopamine-immobilized lysozyme for the fabrication of antibacterial films and its application in the preservation of fresh pork, *Food Packag. Shelf Life*, 2024, **43**, 101288.
34 Z. Hu, S. Li, S. Wang, B. Zhang and Q. Huang, Encapsulation of menthol into cyclodextrin metal-organic frameworks: Preparation, structure characterization and evaluation of complexing capacity, *Food Chem.*, 2021, **338**, 127839.
35 Z. Qin, Q. Jiang, Y. Zou, M. Chen, J. Li, Y. Li and H. Zhang, Synthesis of Nanosized γ-Cyclodextrin Metal-Organic Frameworks as Carriers of Limonene for Fresh-Cut Fruit Preservation Based on Polycaprolactone Nanofibers, *Small*, 2024, **20**(29), 2400399.
36 S. Chen, J. Cao and J. Zheng, Reprocessable Silyl Ether-Based Dynamic Covalent Poly(dimethylsiloxane) Networks with Superb Thermal Stability and Creep Resistance, *ACS Appl. Polym. Mater.*, 2024, **6**, 4215–4225.
37 M. Zhao, Z. Liu, W. Zhang, G. Xia, C. Li, K. Rakariyatham and D. Zhou, Advance in aldehydes derived from lipid oxidation: A review of the formation mechanism, attributable food thermal processing technology, analytical method and toxicological effect, *Food Res. Int.*, 2025, **203**, 115811.
38 S. White, A. Jackson-Davis, K. Gordon, K. Morris, A. Dudley, A. Abdallah-Ruiz, K. Allgaier, K. Sharpe, A. K. Yenduri, K. Green and F. Santos, A Review of Non-thermal Interventions in Food Processing Technologies, *J. Food Prot.*, 2025, **88**(6), 100508.

39 K. Seku, G. Bhagavanth Reddy, A. I. Osman, S. S. Hussaini, N. S. Kumar, M. Al-Abri, B. Pejjai, S. B. Alreshaidan, A. S. Al-Fatesh and K. K. Kadimpati, Modified frankincense resin stabilized gold nanoparticles for enhanced antioxidant and synergetic activity in in-vitro anticancer studies, *Int. J. Biol. Macromol.*, 2024, **278**, 134935.

40 Y. He, X. Wang, C. Zhang, J. Sun, J. Xu and D. Li, Near-Infrared Light-Mediated Cyclodextrin Metal-Organic Frameworks for Synergistic Antibacterial and Anti-Biofilm Therapies, *Small*, 2023, **19**(35), 2300199.

41 H. Zhou, T. Li, E. Zhu, S. Wang, Q. Zhang, X. Li, L. Zhang, Y. Fan, J. Ma and Z. Wang, Dissolving-co-catalytic strategy for the preparation of flexible and wet-stable cellulose film towards biodegradable packaging, *Int. J. Biol. Macromol.*, 2024, **275**, 133454.

42 Y. He, T. Zhong, Y. Liu, M. Wan, L. Sun, Y. Zhao and Z. Wang, Development of a multifunctional active food packaging film based on electrospun polyvinyl alcohol/chitosan for preservation of fruits, *Int. J. Biol. Macromol.*, 2024, **277**, 134636.

43 X. Lan, T. Luo, Z. Zhong, D. Huang, C. Liang, Y. Liu, H. Wang and Y. Tang, Green cross-linking of gelatin/tea polyphenol/ε-poly (L-lysine) electrospun nanofibrous film for edible and bioactive food packaging, *Food Packag. Shelf Life*, 2022, **34**, 100970.

44 C. Gao, P. Chen, Y. Ma, L. Sun, Y. Yan, Y. Ding and L. Sun, Multifunctional polylactic acid biocomposite film for active food packaging with UV resistance, antioxidant and antibacterial properties, *Int. J. Biol. Macromol.*, 2023, **253**, 126494.

45 B. Al-Abdallah, Y. S. Al-Faiyz and S. Shaaban, Anticancer, Antimicrobial, and Antioxidant Activities of Organodiselenide-Tethered Methyl Anthranilates, *Biomolecules*, 2022, **12**(12), 1765.

46 B. Al-Abdallah, Y. S. Al-Faiyz and S. Shaaban, Organoselenocyanates Tethered Methyl Anthranilate Hybrids with Promising Anticancer, Antimicrobial, and Antioxidant Activities, *Inorganics*, 2022, **10**(12), 246.

47 J. Beurton, I. Clarot, J. Stein, B. Creusot, C. Marcic, E. Marchioni and A. Boudier, Long-lasting and controlled antioxidant property of immobilized gold nanoparticles for intelligent packaging, *Colloids Surf., B*, 2019, **176**, 439–448.

48 B. Zhu, N. Xie, L. Yue, K. Wang, M. Z. Bani-Fwaz, H. Hussein Osman, A. F. El-kott and X. Bai, Formulation and characterization of a novel anti-human endometrial cancer supplement by gold nanoparticles green-synthesized using Spinacia oleracea L. Leaf aqueous extract, *Arab. J. Chem.*, 2022, **15**, 103576.

49 F. Pan, M. Liu, S. Altenried, M. Lei, J. Yang, H. Straub, W. W. Schmahl, K. Maniura-Weber, O. Guillaume-Gentil and Q. Ren, Uncoupling bacterial attachment on and detachment from polydimethylsiloxane surfaces through empirical and simulation studies, *J. Colloid Interface Sci.*, 2022, **622**, 419–430.

50 Y. Wen, W. Chen, R. Wu, J. Guo, X. Liu, B. Shi, C. Zhang, L. Wu, Y. Zheng, A. Liu and L. Lin, Chitosan-Stabilized PtAu Nanoparticles with Multienzyme-Like Activity for Mixed Bacteria Infection Wound Healing and Insights into Its Antibacterial Mechanism, *Small Struct.*, 2024, **5**(6), 2300553.

51 J. Xin, Q. Pu, R. Wang, Y. Gu, L. He, X. Du, G. Tang and D. Han, Antibacterial activity and mechanism of chelerythrine against Streptococcus agalactiae, *Front. Vet. Sci.*, 2024, **11**, 1408376.

52 S. Shaaban, A. M. Abu-Dief, M. Alaasar, A. S. Al-Janabi, N. S. Alsadun, O. K. Al Duaij and T. A. Yousef, Novel Fe (III), Cu (II), and Zn (II) Chelates of Organoselenium-Based Schiff Base: Design, Synthesis, Characterization, DFT, Anticancer, Antimicrobial, and Antioxidant Investigations, *Appl. Organomet. Chem.*, 2024, **39**(1), e7776.

53 S. Shaaban, K. T. Abdullah, K. Shalabi, T. A. Yousef, O. K. Al Duaij, G. M. Alsulaim, H. A. Althikrallah, M. M. Alaasar, A. S. Al-Janabi and A. M. Abu-Dief, Synthesis, Structural Characterization, Anticancer, Antimicrobial, Antioxidant, and Computational Assessments of Zinc(II), Iron(II), and Copper(II) Chelates Derived From Selenated Schiff Base, *Appl. Organomet. Chem.*, 2024, **38**(12), e7712.

54 W. S. Hamama, G. G. El-Bana, S. Shaaban and H. H. Zoorob, Synthetic Approach to Some New Annulated 1,2,4-Triazine Skeletons with Antimicrobial and Cytotoxic Activities, *J. Heterocycl. Chem.*, 2018, **55**(4), 971–982.

55 R. Qin, S. Yang, B. Fu, Y. Chen, M. Zhou, Y. Qi, N. Xu, Q. Wu, Q. Hua, Y. Wu and Z. Liu, Antibacterial activity and mechanism of the sesquiterpene δ-cadinene against Listeria monocytogenes, *LWT*, 2024, **203**, 116388.

56 C. Song, S. Luo, M. He, X. Zhao and M. Sun, Antibacterial mechanism of water-soluble CeO_2 nanoflowers and its product design in antibacterial application, *Appl. Surf. Sci.*, 2025, **679**, 161249.

57 A. Baracca, G. Sgarbi, G. Solaini and G. Lenaz, Rhodamine 123 as a probe of mitochondrial film potential: Evaluation of proton flux through F0 during ATP synthesis, *Biochim. Biophys. Acta, Bioenerg.*, 2003, **1606**, 137–146.

58 L. D. Zorova, V. A. Popkov, E. Y. Plotnikov, D. N. Silachev, I. B. Pevzner, S. S. Jankauskas, V. A. Babenko, S. D. Zorov, A. V. Balakireva, M. Juhaszova, S. J. Sollott and D. B. Zorov, Mitochondrial film potential, *Anal. Biochem.*, 2018, **552**, 50–59.

59 A. M. Abdula, G. L. Mohsen, B. H. Jasim, M. S. Jabir, A. I. Rushdi and Y. Baqi, Synthesis, pharmacological evaluation, and in silico study of new 3-furan-1-thiophene-based chalcones as antibacterial and anticancer agents, *Heliyon*, 2024, **10**, e32257.

60 X. Wang, F. Cheng, X. Wang, T. Feng, S. Xia and X. Zhang, Chitosan decoration improves the rapid and long-term antibacterial activities of cinnamaldehyde-loaded liposomes, *Int. J. Biol. Macromol.*, 2021, **168**, 59–66.

61 R. Zheng, G. Liao, J. Kang, S. Xiong and Y. Liu, An intelligent myofibrillar protein film for monitoring fish freshness by recognizing differences in anthocyanin (Lycium ruthenicum)-induced color change, *Food Res. Int.*, 2024, **192**, 114777.

62 S. Zhuang, H. Hong, L. Zhang and Y. Luo, Spoilage-related microbiota in fish and crustaceans during storage:

Research progress and future trends, *Compr. Rev. Food Sci. Food Saf.*, 2020, **20**, 252–288.

63 Y. Yang, X. Yu, Y. Zhu, Y. Zeng, C. Fang, Y. Liu, S. Hu, Y. Ge and W. Jiang, Preparation and application of a colorimetric film based on sodium alginate/sodium carboxymethyl cellulose incorporated with rose anthocyanins, *Food Chem.*, 2022, **393**, 133342.

64 O. Romruen, T. Karbowiak, R. Auras and S. Rawdkuen, Smart bilayer film: Quality monitoring for freshness of fish and minced pork delights, *Food Packag. Shelf Life*, 2024, **44**, 101299.

65 S. You, X. Zhang, Y. Wang, Y. Jin, M. Wei and X. Wang, Development of highly stable color indicator films based on κ-carrageenan, silver nanoparticle and red grape skin anthocyanin for marine fish freshness assessment, *Int. J. Biol. Macromol.*, 2022, **216**, 655–669.

66 N. Wells, D. Yusufu and A. Mills, Colourimetric plastic film indicator for the detection of the volatile basic nitrogen compounds associated with fish spoilage, *Talanta*, 2019, **194**, 830–836.

67 M. Saed, R. D. Ayivi, J. Wei and S. O. Obare, Gold nanoparticles antibacterial activity: Does the surface matter?, *Colloid Interface Sci. Commun.*, 2024, **62**, 100804.

68 A. Khan, P. Ezati and J. Rhim, Chitosan/gelatin-based multifunctional film integrated with green tea carbon dots to extend the shelf life of pork, *Food Packag. Shelf Life*, 2023, **37**, 101075.

69 R. Sasikumar, S. Saranya, L. Lourdu Lincy, L. Thamanna and P. Chellapandi, Genomic insights into fish pathogenic bacteria: A systems biology perspective for sustainable aquaculture, *Fish Shellfish Immunol.*, 2024, **154**, 109978.